# Weakly-supervised temporal segmentation of cell-cycle stages with center-cell focus using Recurrent Neural Networks

Abin Jose[1*], Rijo Roy[1*], Johannes Stegmaier[1]

[1]Institute of Imaging and Computer Vision, RWTH Aachen University, Aachen, Germany
[2]Institute of Biochemistry and Molecular Cell Biology, RWTH Aachen University, Aachen
[*]Authors contributed equally
abin.jose@lfb.rwth-aachen.de

**Abstract.** Training deep-learning models for biomedical images has always been a problem because of the unavailability of annotated training data. Here we propose using a model and a training approach for the weakly-supervised temporal classification of cell-cycle stages during mitosis. Instead of using annotated data, by using an ordered set of classes called transcripts, our proposed approach classifies the cell-cycle stages of cell video sequences. The network design helps to propagate information in time using Recurrent Neural Network layers and helps to focus the features on the center-cell using two loss functions. The proposed system is evaluated on four datasets from LiveCellMiner and has a comparable performance with the supervised approaches, considering the annotated data is not used for training. The predicted classification of the unannotated interphase-recovery class by our approach also aligns with the findings from the LiveCellMiner.

## 1 Introduction

Mitosis is the process by which the cells rearrange and split into two identical daughter cells [1]. It is quite important to study and understand cell division to characterize pathological phenotypes in clinically relevant situations. The cell-cycle is divided into four phases: S, G2, Mitosis, and G1. The G1, S, and G2 phases are referred to as interphase. Mitosis is further classified according to the chromatin morphology into prophase, prometaphase, metaphase, anaphase, and telophase, were the pass to G1 is typically marked at cytoplasmic level by the cytokinetic process, which separates the cell bodies. Here we regard post-mitosis as the period where very gradual changes bring the compact anaphase chromatin to a decondensed G2-like mass in early G1. In this work, we consider the classification of the cell-cycle stages into three different phases as in [2]: interphase, mitosis, and post-mitosis. Current state-of-the-art methods [2, 3] extract hand-engineered features, which are then classified using clustering methods. Zhong et al. [3] proposed an unsupervised clustering algorithm based on a temporally constrained combinatorial clustering (TC3) method. LiveCellMiner [2] additionally uses conventional convolutional networks to extract image features and uses a long short-term memory (LSTM) network to identify erroneous cell-cycle sequences. K-means clustering, after the feature extraction from fluorescence microscopy images, was proposed by Ferro et al. [4] for classification. Many supervised deep learning-based methods [5–9] are available for cell-cycle detection and classification. Recently, Jose et al. proposed

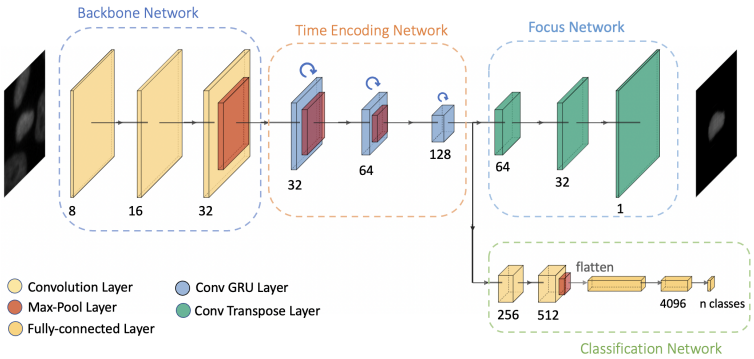


**Fig. 1.** Illustration of our proposed architecture [10]. The model consists of two output networks, a focus network to reconstruct the center-cell and a classification network to classify the images.

a Recurrent Neural Network (RNN) based architecture [10] to incorporate time-related propagation of features for classification. However, this approach is supervised and requires careful annotations by a trained biologist. To overcome this problem, in this paper, we propose a weakly-supervised training scheme. The main advantages of this work are: 1) The network is end-to-end trainable and shallow. 2) The network focuses on the center-cell and occludes neighboring cells. 3) The classification head classifies the different states. 4) The training is weakly-supervised and needs only a transcript, which is a list of classes in order. For example, the transcript for a cell sequence is represented as : [interphase, mitosis, post-mitosis] as in the order of occurrence of classes, and it doesn't need dense image-to-image annotations.

## 2 Materials and methods

### 2.1 Network architecture

For the temporal segmentation of the cell-cycle stages, we propose to use the same architecture as the one proposed in [10], but the training method varies. The architecture of the model is shown in Fig. 1. The model architecture contains four main parts. 1) A backbone network to extract the features, 2) a time encoding network consisting of RNN layers to combine extracted features between the current frame and propagated features from the previous frame, 3) a focus network that helps to focus the extracted features towards the center-cell and 4) a classification network to classify the input sequences into cell-cycle stages. We used convolutional Gated Recurrent Unit (GRU) as the type of RNN because our focus network reconstructs the image from extracted features and helps to focus the features on the center-cell. The network architecture takes an image as the input and has two output networks: the focus network and the classification network. The training of these networks is explained in detail in the next section.

### 2.2 Training details

The proposed model architecture contains RNN layers, which help the flow of information through time for a given input sequence. Thus in this model, the image at each time

frame is dependent on the previous images from the same sequence. Inspired by the Neural Network-Viterbi approach proposed by Richard et al. [11], our approach uses the Viterbi decoding method for the weakly-supervised training. For a given input sequence, given the order of occurrence of classes as a constraint, the weakly-supervised method finds the most probable set of labels. This set of labels contains the most probable class for each image in the input sequence under the given constraint. So, following training, the model gains the ability to recognize the classes for an input sequence given the classes' occurrence order. As mentioned, our model architecture has two main output networks. A focus network to reconstruct the center-cell from the features and a classification network to predict the most probable sequence of labels. The losses from these two networks are trained end-to-end to get the desired output.

**Focus network loss:** The output of the focus network has a dimensionality equal to that of the input images. To reconstruct only the center-cell from the input image, the training calculates the loss between the predicted output and a masked image. This network aims to learn the features corresponding only to the center-cell in the input image and thus focus on the features of the center-cell. The masked image is obtained by using the annotated segmentation mask available with the datasets and setting all pixels that do not belong to the target cell to zero. The last layer of the focus network uses a sigmoid activation layer. The loss between the predicted and the expected input is calculated using binary cross-entropy (BCE) loss [12] as shown below

$$\mathrm{L_{focus}} = \frac{1}{\mathrm{W_0 * H_0}} \sum_{\mathrm{w} \in \mathrm{W_0}} \sum_{\mathrm{h} \in \mathrm{H_0}} \mathrm{BCE}\big(y\,(\mathrm{w}, \mathrm{h})\,, \hat{y}\,(\mathrm{w}, \mathrm{h})\,\big), \tag{1}$$

where $y\,(\mathrm{w}, \mathrm{h})$ and $\hat{y}\,(\mathrm{w}, \mathrm{h})$ are the input and predicted values of the network at pixel location $(\mathrm{w}, \mathrm{h})$. $\mathrm{W_0}$ and $\mathrm{H_0}$ are the input image dimensions. It is also possible to extract the segmentation mask of unseen images from this dataset using a simple threshold operation on the predicted output of the focus network.

**Classification network loss:** The classification network treats the input as a sequence to determine the most probable path of classes. The computation of the most probable path and the loss associated with that path can be calculated only after getting the prediction outputs for all frames in a sequence. The classification network output is the posterior probability, that is the probability of each class given the input image. The Viterbi algorithm [11] finds the most probable path using these posterior probabilities and a length model. Our approach used a class-dependent Poisson distribution as the length model as suggested in the original paper. Once the Viterbi algorithm finds the most probable path of labels, these labels are used to back-propagate through the network. A negative log-likelihood loss is used to train the network. Let the most probable path for an input sequence $\mathrm{x}^T$ found by the Viterbi algorithm be given by $\mathrm{c}_{n(t)}$. Then the weakly-supervised classification loss given by

$$\mathrm{L_{clf}} = -\sum_{t=1}^{T} \log p\left(\mathrm{c}_{n(t)} | \mathrm{x}^{\intercal}\right). \tag{2}$$

**Total training loss:** Both losses are computed for a sequence of data as input. A combined focus loss is obtained by summing the focus losses from every frame. The total loss is computed by a weighted sum of the combined focus loss and the weakly-supervised classification loss. A regularization parameter $\lambda_{\mathrm{reg}}$ is used as the weight.

$$\mathrm{L_{tot}} = \sum_{t=1}^{T} (\mathrm{L_{focus}}) + \lambda_{\mathrm{reg}} \cdot \mathrm{L_{clf}}. \tag{3}$$

### 2.3 Datasets and experiments

**Datsets:** The datasets used for the evaluations are provided by LiveCellMiner [2]. The datasets contain microscopic image sequences of the mitosis process after the cell tracking. The datasets are acquired on human HeLa cells expressing H2B-mCherry transfected with indicated siRNA oligonucleotides in eight-well $\mu$-slide chambers. It contains images that were taken three minutes apart. There are four datasets available from LiveCellMiner, namely LSM710 dataset, LSD1 dataset, RecQL4 dataset, and NikonXLight dataset. The former three datasets are captured using a confocal microscope and the latter is captured using a widefield microscope. Each contained cell is represented by a sequence of 90 frames, cropped to a resolution of $96 \times 96$ pixels with the target cell at the center. The dataset is annotated into three classes such as interphase class, mitosis class (prophase to early anaphase), and post-mitosis class (late anaphase to interphase). The post-mitosis class also contains cells that have grown into interphase (interphase recovery class) after cell division. Our approach is also able to identify the interphase recovery class, but we don't have a valid ground truth to evaluate instead, we qualitatively compared it with the findings from [2].
**Experimental setup:** For training the weakly-supervised model, a set of ordered labels called transcripts are used instead of the annotated data. The transcripts are simply the list of the classes in their order of occurrence. Our approach finds the number of frames in a sequence belonging to each class, given the transcript. Thus it helps to avoid the task of frame-to-frame annotation for training this model and the time involved for it. Given input sequences, the model trains both losses together with a regularization hyperparameter $\lambda_{\text{reg}}$ (selected value is 0.01). The batch size and the learning rate are selected as 4 and 0.01 respectively, and the weakly-supervised classification loss is introduced once every 20 iterations. The length of the transcript used is 4 considering the interphase recovery class as the fourth class. For evaluation with the user annotation the interphase recovery class is considered a part of the post-mitosis class.
**Evaluation criteria:** The annotated data is available with the datasets for evaluation. We have calculated the frame-to-frame accuracy for each sequence and then averaged it. We also calculated the confusion matrix to find the correct classification and the misclassification rates. We compared the performance of our approach and compared the results obtained with the same model architecture trained using supervised methods [10] and the ResNet18 classification model.

### 2.4 Results

We plotted the label matrix in which the x-axis represents the length of each cell sequence, and the y-axis represents different sequences selected from the test dataset. Fig. 2 (a) shows the label matrix of the ground truth annotations compared with the label matrix of the predicted output on 50 test sequences of the LSM710 dataset. On closer inspection, it is evident that the predictions by the proposed model are similar to the user annotations. Fig. 2 (b) shows the first three principal components of the embedding space for the three classes of our proposed model. The embedding space contains the characteristics of the input data, in which the three cell-cycle states are clustered and move from blue to red to pink states and is clearly visible in the feature

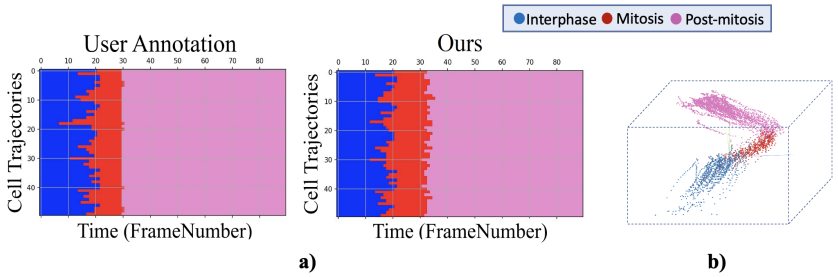


**Fig. 2.** Illustration of the a) label matrix of the predicted output of our proposed approach compared with the user annotation, and b) first three principal components plot of the learned embedding space for the LSM710 dataset.

space. From the figure, it is clear that our proposed weakly-supervised method can cluster the features belonging to different classes without using fully-annotated data for training. Frame-to-frame accuracies can give a better quantitative analysis of the results. Tab. 1 shows the accuracies of the proposed model for the four datasets compared to the supervised learning approach [10] and also the ResNet18 classifier. Even though the proposed model has slightly lower (around 3-4%) accuracies when compared to the supervised methods, the results are extremely good considering that dense ground truth annotations are not required for training. Fig. 3 shows the reconstructed image from the focus network for a given input image. The focus network reconstructs only the center-

| Model | Dataset | | | |
|---|---|---|---|---|
| | LSM710 | LSD1 | RecQL4 | NikonXLight |
| Supervised [10] | 99.544 | 99.074 | 99.316 | 99.112 |
| ResNet18 [10] | 99.301 | 98.995 | 98.614 | 98.696 |
| **Ours** | 96.215 | 94.821 | 98.541 | 96.859 |

**Tab. 1.** The frame-to-frame accuracy values of our proposed model in comparison with the supervised approaches [10] for the four different datasets.

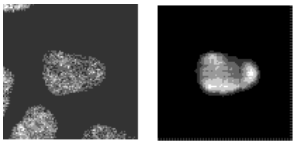

**Fig. 3.** For an input image shown to the left, the output predicted by the focus network is shown to the right.

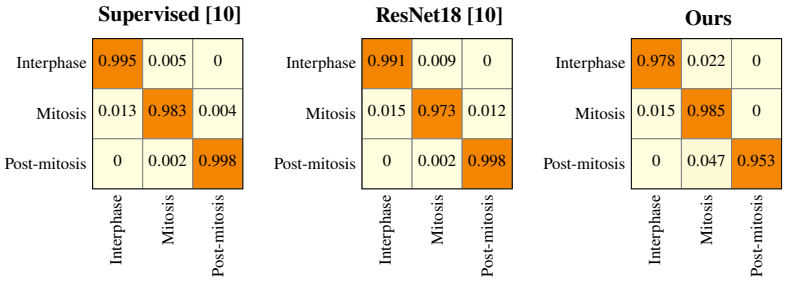


**Fig. 4.** Normalized confusion matrices for the prediction on the LSM710 test dataset with our proposed model compared with supervised approaches [10].

cell and thus helps the features learned in the embedding space to focus on the target cell. A segmentation mask of the target cell can be also predicted from the output of the focus network by using a simple intensity threshold. Fig. 4 illustrates the confusion matrix of the proposed approach compared to the supervised approaches [10]. It is evident from the diagonal elements of the confusion matrix that the correct classification for three different classes is comparable to that with supervised methods. It is observed that the true positive rate for the mitosis class is higher than the other approaches. This indicates that the proposed weakly-supervised method can identify mitosis class images better than supervised approaches. For the other two classes, the misclassification rate is higher for the proposed approach. It is also clear that confusion between unrelated classes does not occur as indicated by the zeros in the top right and the bottom left. Fig. 5 (a) demonstrates a plot from LiveCellMiner [2], which shows interphase recovery for the LSM710 dataset happens around 20 frames after mitosis. Fig. 5 (b) illustrates the label matrix of the proposed model when predicted into four classes. It is evident from this figure that the recovered interphase class (second set of blue) happens after around 20 frames from the mitosis class (red). Even though there are no ground-truth annotations to evaluate an accurate measure, the qualitative results from the proposed model are in alignment with the findings from the LiveCellMiner.

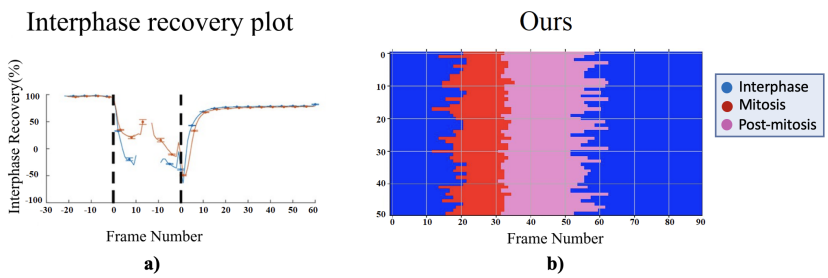


**Fig. 5.** Illustration of the interphase recovery class prediction. a) Plot from the LiveCellMiner [2] illustrates that the interphase recovery occurs after 20 frames from mitosis. b) Our proposed weakly-supervised method when predicted into four classes predicted the recovered interphase frames (second set of blue after pink). The post-mitosis class (pink) happens for around 20 frames.

## 3 Discussion

We propose an automatic method for the identification of cell-cycle stages during mitosis. The proposed weakly-supervised approach only needs the transcript information which indicates the order of occurrence of cell-cycle states. Even though the classification accuracy is slightly lower compared to the supervised RNN model and ResNet18 classifier model, the proposed approach has the advantage that the user needs to provide only the order of occurrence of the states. This avoids the need for the generation of user annotation to train supervised models, which needs the expertise of a trained biologist. In the future, we would like to further extend the experiments to 3D cell datasets. Another interesting research direction is to use unsupervised training methods.

## References


1. Araujo AR, Gelens L, Sheriff RS, Santos SD. Positive feedback keeps duration of mitosis temporally insulated from upstream cell-cycle events. Molecular Cell 64.2 (2016), pp. 362–375.
2. Moreno-Andrés D, Bhattacharyya A, Scheufen A, Stegmaier J. LiveCellMiner: A new tool to analyze mitotic progression. PloS One 17.7 (2022), e0270923.
3. Zhong Q, Busetto AG, Fededa JP, Buhmann JM, Gerlich DW. Unsupervised modeling of cell morphology dynamics for time-lapse microscopy. Nature Methods 9.7 (2012), pp. 711–713.
4. Ferro A, Mestre T, Carneiro P, Sahumbaiev I, Seruca R, Sanches JM. Blue intensity matters for cell cycle profiling in fluorescence DAPI-stained images. Laboratory Investigation 97.5 (2017), pp. 615–625.
5. Allehaibi KHS, Nugroho LE, Lazuardi L, Prabuwono AS, Mantoro T et al. Segmentation and classification of cervical cells using deep learning. IEEE Access 7 (2019), pp. 116925–116941.
6. Narotamo H, Fernandes MS, Moreira AM, Melo S, Seruca R, Silveira M et al. A machine learning approach for single cell interphase cell cycle staging. Scientific Reports 11.1 (2021), pp. 1–13.
7. Jin X, Zou Y, Huang Z. An imbalanced image classification method for the cell cycle phase. Information 12.6 (2021), p. 249.
8. Saha M, Chakraborty C, Racoceanu D. Efficient deep learning model for mitosis detection using breast histopathology images. Computerized Medical Imaging and Graphics 64 (2018), pp. 29–40.
9. Albayrak A, Bilgin G. Mitosis detection using convolutional neural network based features. 2016 IEEE 17th International Symposium on Computational Intelligence and Informatics (CINTI). IEEE. 2016, pp. 000335–000340.
10. Jose A, Roy R, Eschweiler D, Laube I, Azad R, Moreno-Andrés D et al. End-To-End Classification Of Cell-Cycle Stages With Center-Cell Focus Tracker Using Recurrent Neural Networks. https://www.biorxiv.org/content/10.1101/2022.11.01.514198v1. 2022.
11. Richard A, Kuehne H, Iqbal A, Gall J. Neuralnetwork-viterbi: A framework for weakly supervised video learning. Proceedings of the IEEE Conference on Computer Vision and Pattern Recognition. 2018, pp. 7386–7395.
12. Ho Y, Wookey S. The real-world-weight cross-entropy loss function: Modeling the costs of mislabeling. IEEE Access 8 (2019), pp. 4806–4813.